https://dx.doi.org/10.21577/0103-5053.20230027

J. Braz. Chem. Soc., Vol. 34, No. 8, 1139-1153, 2023

Article

Dereplication of Sclerotiorin-Like Azaphilones Produced by *Penicillium meliponae* Using LC-MS/MS Analysis and Molecular Networking

Eldrinei G. Peres, [a] ***Mayane P. Souza,*** [b] ***Thiago F. Sousa,*** [a,c] ***Carlos V. A. da Silva,*** [a] ***André L. Barros,*** [a] ***Felipe M. A. da Silva,*** [d] ***Emmanoel V. Costa,*** [b] ***Lívia S. de Medeiros,*** [e] ***Moacir R. Forim,*** [f] ***Afonso D. L. de Souza,*** [b] ***Weider H. P. Paz,*** [a] ***Gilvan F. da Silva,*** [c] ***Antonia Q. L. de Souza*** [g] ***and Hector H. F. Koolen*** [*,a]

[a]*Grupo de Pesquisas em Metabolômica e Espectrometria de Massas, Universidade do Estado do Amazonas, 69080-900 Manaus-AM, Brazil*

[b]*Departamento de Química, Universidade Federal do Amazonas, 69067-005 Manaus-AM, Brazil*

[c]*Embrapa Amazônia Ocidental, 69010-970 Manaus-AM, Brazil*

[d]*Centro de Apoio Multidisciplinar, Universidade Federal do Amazonas, 69080-900 Manaus-AM, Brazil*

[e]*Instituto de Ciências Ambientais Químicas e Farmacêuticas, Universidade Federal de São Paulo, 09972-270 Diadema-SP, Brazil*

[f]*Departamento de Química, Universidade Federal de São Carlos, 13565-905 São Carlos-SP, Brazil*

[g]*Faculdade de Ciências Agrárias, Universidade Federal do Amazonas, 69080-900 Manaus-AM, Brazil*

Penicillium meliponae, a recently described and rare species, was isolated as an endophytic fungus from the Amazonian plant *Duguetia sthelechantha*, and has been proven to be a pigment producer. Considering the high productivity of this species and the lack of data on its chemical composition, the present study aimed to characterize the chemical profile of *P. meliponae* and evaluate the influence of agitation and the use of different culture media. For this purpose, liquid chromatography coupled with mass spectrometry (LC-MS/MS) and molecular networking were used, allowing the identification of 17 azaphilone molecules with sclerotiorin-like skeletons, becoming the first chemical report of this species. In addition, the different production patterns in the tested culture media were indicative that this species is sensitive to changes in the composition of the carbon source and to the presence of agitation. Furthermore, this work contributes to the fragmentation mechanisms of the different possible structural arrangements for azaphilones of the sclerotiorin type and serves as a repository of information on the gas-phase behavior of this type of metabolite in mass spectrometry experiments and will assist future studies aimed at the discovery of azaphilones.

Keywords: *Penicillium meliponae*, OSMAC, azaphilones, molecular networking, LC-MS/MS

Introduction

The Amazon rainforest is home to an enormous biodiversity,[1,2] still little known and explored. Within this biodiversity, microorganisms play a vital role in the maintenance of the biome, of which fungi have a prominent role, since they contribute to the recycling of organic matter.[3,4] These organisms are ubiquitous in the Amazon biome, and can be found in sediments, in water and in association with animals and plants (endophytic).[5,6] In particular, the different types of endophytic fungi found in the Amazon have become the result of numerous studies, among them the genus *Penicillium* due to its metabolic capacity and high recurrence in isolation studies.[7-9] This genus comprises cosmopolitan filamentous

*e-mail: hkoolen@uea.edu.br
Editor handled this article: Emanuel Carrilho (Associate)

fungi[10] and, according to recent literature, it contains about 483 cataloged specimens distributed worldwide.[11] Fungi of the genus *Penicillium* are capable of producing a range of structurally diverse compounds with various reported bioactivities, which include antimicrobial, anti-inflammatory, anticancer, antioxidant, enzyme inhibitory and cytotoxic properties.[12-14] Among the various classes of secondary metabolites produced by *Penicillium*, polyketides can be highlighted due to their high number of structures described, as well as their biotechnological potential.[14]

Within the group of polyketides, substances of the subclass of azaphilones constitute a large group of pigments that structurally share the presence of a bicyclic pyranquinone nucleus, which is highly oxygenated and highly reactive in the presence of ammonia; a characteristic that gave rise to the name of the class.[15,16] Azaphilones have several biological activities that include antimicrobial,[17-20] antiviral,[21-23] cytotoxic,[22,24,25] anticancer[22,26-28] and anti-inflammatory properties.[29-31] Among the genera that produce molecules of this class, *Penicillium* stands out as the largest producer, followed by *Monascus*, *Talaromyces*, *Aspergillus*, *Colletotrichum*, *Fusarium*, and *Chaetomium*, among others.[15,16] Within the genus *Penicillium*, several species have been reported as producers of the most diverse types of azaphilones, of which the citrinin and sclerotiorin groups stand out.[15,16]

In addition to their potential for the development of new drugs, azaphilones can be employed as food dyes, such as those derived from *Monascus* species and which are used in the Asian market.[32] Regarding the use of new productive strains, a recurring concern is the ability to produce the mycotoxin citrinin, which is an agent with nephrotoxic, hepatotoxic and cytotoxic effects.[32] In this sense, the investigation of new productive strains through the "omic" sciences is fundamental since, by establishing the genetic and metabolic diversity of azaphilone-producing fungi, it is possible to evaluate the production of undesirable molecules, as well as provide a chemical profile of those that are potentially useful for future uses of the strains.[33]

As such, by means of liquid chromatography coupled to sequential mass spectrometry (LC-MS/MS) and molecular networks, this work sought to characterize the chemical profile of the azaphilones produced by *Penicillium meliponae*, which is a fungus that has recently been described in the literature,[34] that has no previous chemical studies and which, in this work, is described and reported here as an endophyte isolated for the first time from the Amazonian rainforest.

Experimental

Origin of the strain

Penicillium meliponae MMSRG058 (SisGen Register AA7741B) was originally isolated from the trunk of the plant *Duguetia sthelechantha*, which was obtained at the Experimental Farm of the Federal University of Amazonas (2°38'44.2" S, 60°03'37.9" W) and deposited in the collection of microorganisms of the Laboratory of Bioassays and Microorganisms of the Amazon (LABMICRA) under the code DgC32.2. Subsequently, the strain was assigned to the mycology collection of the Metabolomics and Mass Spectrometry Research Group of the Amazonas State University, under the code MMSRG058.

Species identification

The isolate MMSRG058 was cultivated in potato-dextrose (PD) liquid culture media (potato 20 g L^{-1}; dextrose 20 g L^{-1}) (Dinâmica, Indaiatuba, SP, Brazil) for four days to obtain the mycelial mass. The broth was filtered, and the deoxyribonucleic acid (DNA) extraction performed using 2% cetyltrimethylammonium bromide cationic detergent (Serva, Osasco, SP, Brazil).[35] The quality of the DNA was verified using a NanoDrop® spectrophotometer (Thermo Fisher, Waltham, Massachusetts, USA) and the integrity was verified via electrophoresis in a 0.8% agarose gel (Kasvi, São José dos Pinhais, PR, Brazil).

The reactions were prepared with the Easytaq® kit (Sinapse Biotecnologia, SP, Brazil). The polymerase chain reaction (PCR) conditions for amplification of the four primers: internal transcribed spacer (ITS), β-tubulin (*benA*), calmodulin-like protein (*cam*) and RNA polymerase II gene (*rpb2*) were the following: initial denaturation at 95 °C for 3 min, 35 cycles with denaturation at 95 °C for 45 s, annealing temperature 55 °C for 45 s, followed by extension at 72 °C for 1 min and final extension 72 °C for 5 min. PCR products were resolved on agarose gel stained with ethidium bromide (Amresco, Solon, OH, USA), photodocumented using a molecular imaging system by Loccus Biotechnologic L-Pix. Chemi (Cotia, SP, Brazil), and the size of the amplicon was compared with the marker 1 kb plus (Invitrogen, Waltham, MA, USA).

For sequencing by the Sanger method, PCR products were purified with Exosap (Applied Biosystems, Waltham, MA, USA). The sequencing reactions were performed in an aliquot of 10 μL, containing 2 μL of ultrapure H_2O, 1.5 μL of Big Dye buffer, 0.5 μL of Big Dye Terminator v3.1 (Thermo Fisher, Waltham, MA, USA), 1 μL of each primer and 5 μL of the purified PCR products. The following

cycling conditions were utilized: 96 °C for 1 min, followed by 35 cycles at 96 °C for 15 s, 50 °C for 15 s and 60 °C for 4 min. Sequencing was performed using a genetic analyzer (3500 series, Thermo Fisher).

Consensus sequences were obtained based on alignment of forward and reverse sequences using DNA baser assembly software.[36] The new sequences obtained were deposited in GenBank[37] under accession numbers: OP374460 (ITS), OP382213 (*cam*), OP382212 (*rpb2*), OP382211 (*benA*). Phylogenetic identification of this strain was performed using a dataset of 35 *Penicillium* sequences from the Sclerotiorum section, and *Penicillium griseola* was used as an outgroup. The sequences of *tub2*, *cam*, *rpb2* were individually aligned with the MAFFT tool in the UGENE software.[38] Alignments were plotted in IQ-Tree 2[39] and a phylogenetic analysis using maximum likelihood (ML) was performed from a concatenation of the *benA*, *cam*, *rpb2* sequences. Bayesian inference (BI) was performed using CIPRES[40] (Figure S1, Supplementary Information (SI) section).

The ML analysis included 1,000 replicates (bootstrap) using all sites, with the best model selected by IQ-Tree. BI was based on the model adopted in PAUP*4 and Mrmodeltest2 v2.[41] All sites in the loci were considered; the analysis was performed for ten million generations, with the first 25% of the trees discarded and burned using the MrBayes v 3.7 tool available from CIPRES.[40] Posterior probability (PP) and tree topology were visualized with Figtree v1.3.2.[42] The consensus tree of the ML and BI analyses was generated manually from the topology obtained by Figtree in BI analysis with the posterior probability values, plus the bootstrap values generated by the maximum likelihood analysis, using the CorelDraw[43] editing package.

Cultivation of the strain and production of extracts

For the cultivation and liquid-liquid partition processes, the following chemical products were used: anhydrous glucose, potassium chloride and soluble starch from Dinâmica (Indaiatuba, SP, Brazil); yeast extract powder and meat extract powder from Himedia (Mumbai, India); hydrated iron(II) sulfate, sodium nitrate and magnesium sulfate from Biotec (Pinhais, PR, Brazil); anhydrous potassium phosphate dibasic was from Vetec (Duque de Caxias, RJ, Brazil); malt extract from Kasvi (São José dos Pinhais, PR, Brazil) and ethyl acetate (AcOEt) from Nuclear (Diadema, SP, Brazil).

The isolate MMSRG058 was cultivated using the one strain-many compounds (OSMAC) approach,[44] in potato-dextrose-yeast (PDY) culture media (3 g of anhydrous glucose, 0.3 g of yeast extract powder, 150 mL of potato water), Czapek (1.5 g of anhydrous glucose, 0.0015 g of hydrated iron(II) sulfate, 0.45 g of sodium nitrate, 0.15 g of anhydrous potassium phosphate dibasic, 0.075 g of magnesium sulfate, 0.075 g of potassium chloride and 150 mL of distilled water), International *Streptomyces* Project 2 (ISP2) (0.6 g of soluble starch, 0.6 g of yeast extract powder, 1.5 g of malt extract and 150 mL of distilled water) and meat medium (ME) (3 g of anhydrous glucose, 0.75 g of meat extract powder and 150 mL of distilled water) in triplicate. Cultures were maintained at 26 °C, and the influence of higher oxygenation (shaking at 180 rpm) and low oxygenation (static) was evaluated for 28 days.

For the separation of the mycelium from the fermented broth, vacuum filtration was performed. AcOEt was used to extract the secondary metabolites from the liquid media via liquid-liquid partition procedure (1 × 125 mL, 1:1 v/v). The solvent was removed from the samples by vacuum rotoevaporation (rotation of 70-80 rpm and temperature between 40-50 ºC; Fisatom, model 803, São Paulo, SP, Brazil) and the extracts were placed in desiccators containing granular silica for the drying process and, subsequently, the extracts obtained in triplicate were pooled for the analysis by LC-MS/MS.

Analysis using LC-MS

Methanol (MeOH), acetonitrile (ACN) and formic acid were purchased from Merck (Darmstadt, Germany). The samples were solubilized in 1 mL of HPLC grade MeOH and centrifuged at 13,000 rpm for 10 min. The supernatant was transferred to 1.5 mL vials, and each sample was subsequently analyzed in a high-performance liquid chromatography system coupled to high resolution mass spectrometry (HPLC-HRMS). The equipment comprises a Nexera X2 liquid chromatograph (Shimadzu, Kyoto, Japan) with diode array detector (DAD)-SPD M20A coupled to a spectrometer with quadrupole-time-of-flight (QTOF), MicroTOF-QII (Bruker Daltonics, Bremen, Germany), equipped with an electrospray source (ESI), operating in positive ionization mode, with an ion transfer time of 70 µs and prepulse of 5 µs. The mass range selected was *m*/*z* 50-1200, AutoMS mode, with collision energy ranging from 20-65 eV according to *m*/*z* 50-700, and with the energy constant at 65 eV for mass values above *m*/*z* 700. A maximum of five precursor ions were acquired *per* cycle. The operating parameters of the equipment were the following: capillary 4500 V, nebulizer gas (nitrogen) 4 bar, drying gas (nitrogen) 9 L min^{-1}, source temperature 200 °C. For internal calibration of the system, 10 nM sodium formate solution in isopropanol/water (1:1 v/v)

was used. For chromatographic separation, a Kinetex C18 analytical column (100 × 2.1 mm, 2.6 µm) (Phenomenex, Torrance, CA, USA), maintained at 50 °C, was used with a flow rate of 0.35 mL min^{-1}. The mobile phase (A) consisted of deionized water, while phase (B) consisted of ACN, both HPLC grade and containing 20 mM of formic acid as an additive. Initially, 15% isocratic elution of (B) was applied for 2 min, with subsequent gradient elution from 15% to 95% of (B) during 2-15 min and a repeated 95% isocratic elution of (B) for 15-21 min. For sample injection, a volume of 10 µL was used. Mass spectra were visualized using DataAnalysis 4.2 software (Bruker Daltomics).[45]

Construction of molecular networks and azaphilone annotation

The MS/MS data obtained was initially converted to the mzXML format with MS-Convert 3.0.21132 software[46] and loaded on the Global Natural Product Social Molecular Networking (GNPS) platform,[47] using the classical mode to construct the molecular networks.[48] The parameters were defined as follows: precursor ion mass tolerance of 0.05 Da, product ion tolerance of 0.1 Da, the cosine of 0.6 with a minimum of six ions for corresponding fragments; each node being able to have a maximum of 10 neighboring nodes connected with at least two nodes *per* cluster and a maximum of 100 nodes connected. Finally, the data were visualized in Cytoscape 3.7.0 software.[49] The molecular network used accessed on the website[47] and the data are publicly available on the MassIVE[50] repository through the code MSV000091281.

The dereplication of known molecules, as well as the identification of new molecules, was performed through the analysis of molecular networks[48] and the manual interpretation of MS/MS spectra, which were compared with The Natural Products Atlas[51] and METLIN[52] databases.

Results and Discussion

Metabolic profile of *P. meliponae* cultures

The OSMAC is a way of diversifying the metabolic capacity of a microorganism strain, either by unlocking cryptic genes or by providing specific substrates that will be incorporated into the produced metabolites.[44,53] Among the various types of metabolic diversification in a microorganism, variation of the composition of the culture medium is presented as a simple and low-cost alternative, and has been applied in many studies.[54,55] In this sense, the variation in the composition of the culture media and the use of agitation or no agitation were evaluated in relation to the capacity to produce secondary metabolites from the fungus *P. meliponae* MMSRG058.

The composition of the culture media and agitation made it possible to considerably expand the metabolic diversity of this strain. In particular, it mainly consisted of different azaphilone analogues, of which 17 different analogues were identified,[33] including geumsanol A (**1**), geumsanol C (**2**), geumsanol B (**6**), isochromophilone VI (**9**), isochromophilone IX (**10**), penazaphilone F (**11**), sclerotioramine (**12**), penazaphilone A (**13**), dechloroisochromophilone II (**14**), ochrephilone (**15**), isorotiorin (**16**) and sclerotiorin (**17**). Initially, the effect of the culture media was compared and the variation in the primary carbon source affected the amount of azaphilones produced. In general, it was observed that the diversity of different analogues of this class ranged from 8 to 16 molecules *per* extract. Of these, the ISP2 medium stood out with the greatest variability of azaphilones that could be identified, with 16 molecules. On the other hand, the Czapek medium had a lower number of these substances (Table 1). Similarly, PDY, ISP2 and meat media enabled the production of compounds containing hydroxyl groups at C-7, C-8, C-11 and C-12 (compounds **1** and **2**), non-chlorinated compounds containing ketone groups at C-8 (compound **5**), chlorinated compounds (compounds **8** and **9**), with the ISP2 medium being the largest producer of the latter, including the production of compounds **4**, **7**, **10**, **11**, **12**, **13** and **17**. In addition to these observations, it was also noticed that the production of some molecules was not feasible when using a certain carbon source. Of these, compound **8** (*m/z* 448.1506) and **13** (*m/z* 504.2128) could not be produced in a media with dextrose as the sole carbon source (Czapek medium), while compound **16** (*m/z* 381.1684), analogue containing a lactone ring as part of its structure, was not observed in the starch-rich ISP2 media (Table 1). Culture media are important factors when the objective is to influence the metabolism of microorganisms and obtain diversity of secondary metabolites, mainly with different carbon sources, as in addition to providing the basis for primary metabolism in heterotrophic organisms, it also provides units of carbon for the biosynthesis of different secondary metabolites.[53]

Finally, regarding agitation, contrasting results were observed. Agitation increased the metabolic diversity of azaphilones in a media with a less complex carbon source (PDY, ISP2 and meat), while decreased the variety of azaphilones in complex media (Czapek). The presence of agitation enabled the production in Czapek medium of compounds containing hydroxyl groups at C-7, C-8, C-11 and C-12 and increased the production of compounds containing a ketone group at C-8. In PDY and

Table 1. Dereplicated molecules from *Penicillium meliponae*

Compound	t_R / min	*m/z* $[M + H]^+$	Chemical formula	Error / ppm	PDY		Czapek		ISP2		Meat	
					SL1	SL2	SL1	SL2	SL1	SL2	SL1	SL2
1 (geumsanol A)	4.9	351.1799	$C_{19}H_{26}O_6$	–2.56	yes[a]	yes	no[b]	yes	yes	yes	yes	yes
2 (geumsanol C)	5.0	353.1958	$C_{19}H_{28}O_6$	–1.70	yes	yes	no	yes	yes	yes	yes	yes
3	5.7	391.2135	$C_{22}H_{30}O_6$	3.58	yes	yes	yes	yes	yes	yes	no	yes
4	6.3	425.1735	$C_{22}H_{29}ClO_6$	0.94	no	yes	no	yes	yes	yes	no	yes
5		373.2027	$C_{22}H_{28}O_5$	3.22	yes	yes	no	yes	yes	yes	yes	yes
6 (geumsanol B)	6.4	417.1926	$C_{23}H_{28}O_7$	3.12	yes	no	yes	yes	yes	yes	yes	yes
7	7.0	505.1722	$C_{25}H_{29}ClN_2O_7$	–3.96	no	no	no	no	yes	no	yes	no
8	7.4	448.1506	$C_{23}H_{26}ClNO_6$	–4.68	yes	no	no	no	yes	no	yes	no
9 (isochromophilone VI)	7.8	434.1726	$C_{23}H_{28}ClNO_5$	–1.84	yes	yes	yes	yes	yes	yes	yes	yes
10 (isochromophilone IX)		476.1848	$C_{25}H_{30}ClNO_6$	1.68	no	no	no	yes	yes	no	no	no
11 (penazaphilone F)	8.1	490.2003	$C_{26}H_{32}ClNO_6$	1.43	no	yes	no	no	yes	yes	no	no
12 (sclerotioramine)		390.1464	$C_{21}H_{24}ClNO_4$	–2.05	yes	yes	yes	yes	yes	yes	yes	yes
13 (penazaphilone A)	9.0	504.2128	$C_{27}H_{34}ClNO_6$	–4.96	no	yes	no	no	yes	no	yes	no
14 (dechloroisocromophilone II)	9.2	357.2073	$C_{22}H_{28}O_4$	1.96	yes	yes	yes	yes	yes	yes	yes	yes
15 (ochrephilone)	9.5	383.1857	$C_{23}H_{26}O_5$	–0.26	yes	yes	yes	yes	yes	yes	yes	yes
16 (isorotiorin)	10.0	381.1684	$C_{23}H_{24}O_5$	–4.72	yes	no	yes	no	no	no	yes	no
17 (sclerotiorin)	10.1	391.1331	$C_{21}H_{23}ClO_5$	4.86	yes	no	yes	yes	yes	no	yes	yes

[a]Present in the assayed condition; [b]not present in the assayed condition. t_R: retention time; PDY: potato-dextrose-yeast; ISP2: International *Streptomyces* project 2; SL1: static liquid; SL2: shaken liquid.

Czapek, agitation increased the production of chlorinated compounds, but decreased in ISP2 and meat media. Also, agitation decreased the production of lactone containing compounds in PDY, Czapek and meat media. Furthermore, it was observed that in some media the use of agitation enabled the production of certain metabolites such as PDY medium (compounds **4**, **11** and **13**), Czapek (compounds **1**, **2**, **4**, **5** and **10**) and meat (compounds **3** and **4**), while it prevented the production of other compounds. Regarding the latter, *P. meliponae* could not produce compounds **6**, **8**, **16** and **17** in PDY media, compound **16** in Czapek, compounds **7**, **8**, **10**, **13** and **17** in ISP2 and compounds **7**, **8**, **13** and **16** in meat (Table 1).

These results show that the physical stress generated by agitation influences the production of azaphilones by *P. meliponae*, suggesting that to obtain a greater diversity of these compounds, static cultivation is more appropriate or, depending on the compound of interest, agitated cultivation should be used. Agitation is one of the important variables in the OSMAC approach in an attempt to promote a change in the metabolic profile of microorganisms,[56] increase metabolic diversity[57] and the production of a specific metabolite of interest.[58,59] Agitation has the purpose of maintaining the homogeneity of the culture medium[60] and increasing the availability of oxygen, facilitating aeration and oxygen absorption and, consequently, influencing the growth of fungi and the production of metabolites.[57]

In general, it was observed that the use of different carbon sources, as well as the use or not of agitation provided metabolic diversification, and it also made it possible for different substances to be produced by a single fungal strain. However, a direct correlation between the composition of the medium and an increase in metabolic capacity is not a direct observation. That is, a more nutrient-rich medium or one with more complex sources of carbon will not necessarily lead to a greater variety of metabolites in *P. meliponae*. Despite the limited number of variables (culture medium and agitation) in the OSMAC approach used, it was possible to observe that the production of azaphilones by *P. meliponae* was directly affected by the cultivation conditions used, increasing or decreasing in some cases the biosynthesis of compounds with characteristic structural skeletons, and that the use of other variables could potentiate the production of azaphilones of interest. The biosynthetic plasticity of this fungal strain is a point to be explored, aiming at the production of substances with different structural skeletons and with possible bioactive potential.

Identification of the azaphilones

The identification of analogues in each extract was performed through manual interpretation of product ion scanning spectra (MS/MS) present in each condition tested,

together with data processing via molecular networks. To facilitate this process, data from sclerotioramine (**12**) (9.0 mg)[61] was used. This molecule served as a "seed" for the propagation of the detection and characterization of the metabolic profile of *P. meliponae* in the different culture media tested (Figure 1 and Figures S2, S3 and S4 and Table S1, SI section). From the LC-MS/MS data processing,[33] molecular families[62] were generated, of which three (A-C) presented azaphilones (Figure S7, SI section). Once the network was created, other analogues showed a similar fragmentation profile to the azaphilones spectra present in the GNPS databases, so compounds **2**, **9**, **10**, **12**, **15** and **17** were characterized directly through the GNPS library (Figures S8-S13, SI section), while the others were propagated through spectral correlation between their chemical structures and connection between nodes.

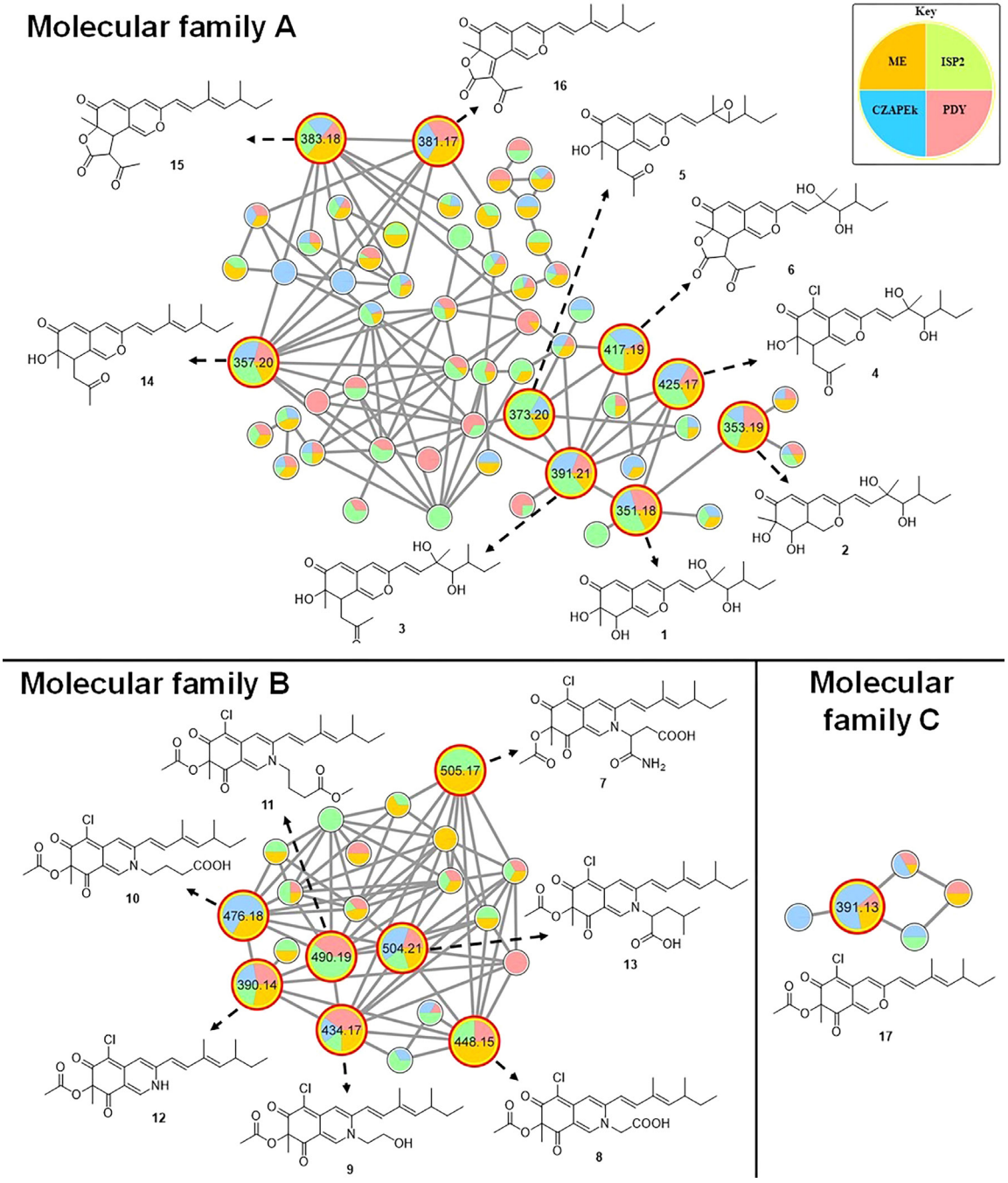

Figure 1. Annotation of molecules in the molecular network. The molecules (nodes) that present spectral similarity are connected by means of edges (gray color) and the level of spectral similarity is given by cosine. The highlighted nodes indicate the *m/z* ratio (protonated molecule) and their relative concentrations (pie chart) in each culture medium in which each annotated molecule was produced. Slices in pink (PDY medium), blue (Czapek medium), green (ISP2 medium) and orange (ME medium). Nodes without *m/z* values refer to ion source fragments, chimeric ions and/or unknown compounds.

In molecular family A (Figure 1), analogs containing oxygen as a heteroatom in the pyran-quinone nucleus were mostly detected, some of which had a chlorine atom in the C-5 position in their structure. However, in molecular family B, nitrogen analogs were identified, and all presented a chlorine atom at C-5. In addition to these, in molecular family C, only compound **17** was identified. Regarding the annotation level, compound **12** was annotated at level 1 (isolated and characterized compounds).[63] All other compounds were annotated at level 2 (which was performed by visualization of molecular families, comparison with databases (when applicable) and manual interpretation of MS/MS spectra).[63] Regarding the annotation, for a better validation of the compounds, plausible fragmentation mechanisms are proposed.

Initially, the fragmentation mechanism of compound **12** (*m/z* 390.1464 $[M + H]^+$, $C_{21}H_{24}ClNO_4$, −2.05 ppm, cos = 0.93) (Figures 2 and S25, SI section) was analyzed. In its product ion scan spectra, several fragment ions resulting from characteristic losses are observed,[33] which are related to functional groups present in sclerotiorin-type azaphilones, such as losses of carbon monoxide (CO, −28 u) and water (H_2O, −18 u).[33,64] Regarding the mechanism, initially fragmentation is observed in the acetyl group connected to the carbon C-7, for which two competitive fragmentations are possible, i.e., the loss of a ketene group (C_2H_2O, −42 u, *m/z* 390 → *m/z* 348, favored) and the neutral loss of acetic acid ($C_2H_4O_2$, −60 u, *m/z* 390 → *m/z* 330) through inductive simple cleavage.[33,64] Additionally, the *m/z* 330 ion can also be formed by the loss of water from the *m/z* 348 fragment

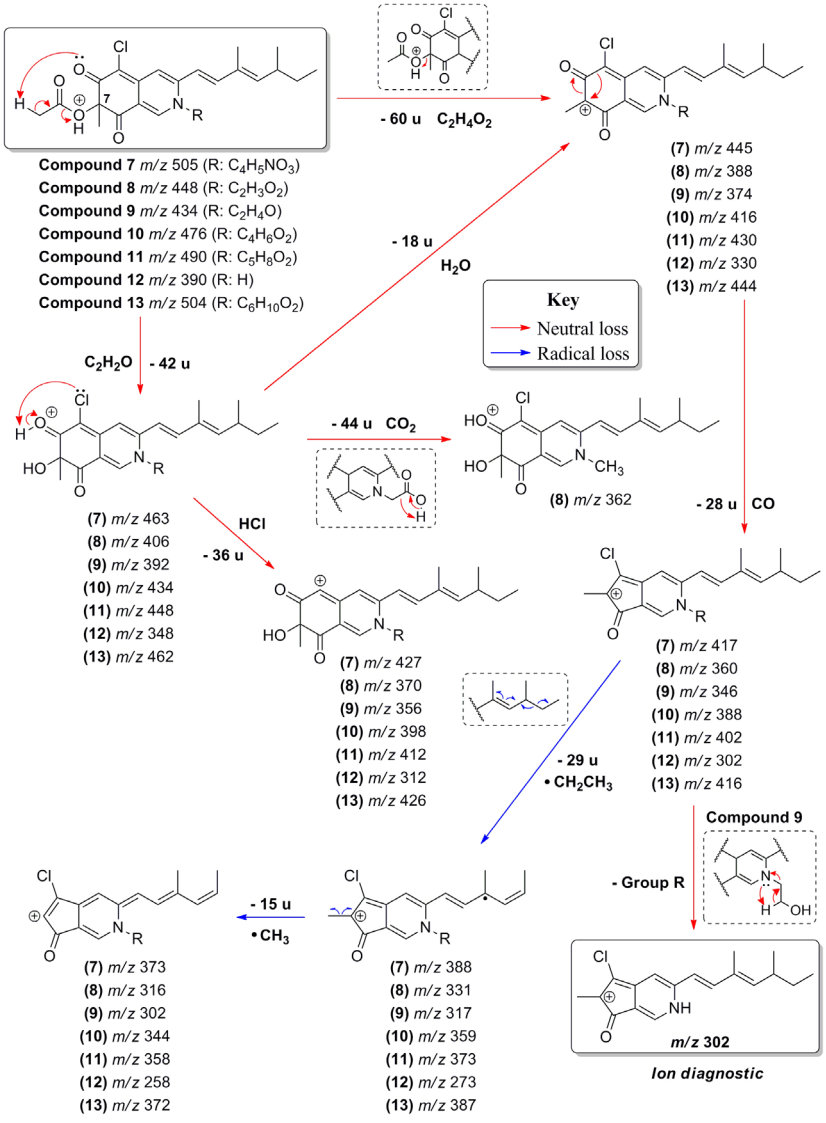

Figure 2. Fragmentation of sclerotiorin analogs. The ion *m/z* 302 is a diagnostic ion and can be formed from the neutral loss of different substituents in nitrogen. Curved arrows indicate the proposed fragmentation mechanisms. Red arrows with full head indicate mechanisms that involve heterolytic cleavages and result in neutral losses. Blue arrows with half a head indicate mechanisms that involve homolytic cleavages and result in radical losses.

(H_2O, −18 u, *m/z* 348 → *m/z* 330). With respect to this last fragment, it can undergo the elimination of hydrochloric acid (HCl) through a proposed mechanism between the chlorine atom and the adjacent protonated carbonyl, which leads to the formation of vinyl cation of *m/z* 312 (HCl, −36 u, *m/z* 348 → *m/z* 312) (Figure 2).

Another important neutral loss observed was the charge-directed loss of CO for allylic cation formation, which can be stabilized by allylic isomerization (*m/z* 330 → *m/z* 302, base peak). Therefore, the formation of smaller fragment ions is proposed from homolytic mechanisms that result in radical losses characteristic of aliphatic chains.[64-66] Of these, the loss of ethyl radical (C_2H_5, −29 u, *m/z* 302 → *m/z* 273) in the side chain is cited, resulting in the formation of distonic ion,[67] in which the fragment can be stabilized by radical allylic isomerization, followed by loss of methyl radical (CH_3, −15 u, *m/z* 273 → *m/z* 258) with formation of vinyl cation (Figure 2). The other annotated analogs have different substituent groups attached to the nitrogen heterocycle allowing losses of different fragments.

In the fragmentation route proposed for compound **9** (*m/z* 434.1726 $[M + H]^+$, $C_{23}H_{28}ClNO_5$, −1.84 ppm, cos = 0.74) (Figure 2), in addition to the losses described above for compound **12**, it had loss of the alcoholic portion present in the structure as enol for formation of the ion *m/z* 302 (C_2H_4O, −44 u, *m/z* 346 → *m/z* 302), by means of a mechanism that involves the capture of a hydrogen-β by the nitrogen free pair of electron with subsequent cleavage of the C–N bond.[64] This proposed mechanism has also been observed in the other analogs for the formation of the ion *m/z* 302. Compound **10** (*m/z* 476.1848 $[M + H]^+$, $C_{25}H_{30}ClNO_6$, 1.68 ppm, cos = 0.64) (Figure S23, SI section) loss an acidic portion ($C_4H_6O_2$, −86 u, *m/z* 388 → *m/z* 302) and compound **11** (*m/z* 490.2003 $[M + H]^+$, $C_{26}H_{32}ClNO_6$, 1.43 ppm, cos = 0.73) (Figure S24, SI section) with the loss of an ester-containing portion ($C_5H_8O_2$, −100 u, *m/z* 402 → *m/z* 302). For compound **8** (*m/z* 448.1506 $[M + H]^+$, $C_{23}H_{26}ClNO_6$, −4.68 ppm, cos = 0.71) (Figure S21, SI section), the loss of the acidic substituent containing only two carbon atoms is proposed with the loss of carbon dioxide (CO_2, −44 u)[68] and formation of the ion *m/z* 362 (*m/z* 406 → *m/z* 362) (Figure 2).

From compound **9**, two analogs were also identified; compound **7** (*m/z* 505.1722 $[M + H]^+$, $C_{25}H_{29}ClN_2O_7$, −3.96 ppm, cos = 0.81) (Figure S20, SI section) with uneven neutral loss, which is indicative of the presence of nitrogen in the fragment ($C_4H_5NO_3$, −115 u, *m/z* 417 → *m/z* 302) and compound **13** (*m/z* 504.2128 $[M + H]^+$, $C_{27}H_{34}ClNO_6$, −4.96 ppm, cos = 0.82) (Figure S26, SI section),[69] with loss of the acid substituent ($C_6H_{10}O_2$, −114 u, *m/z* 416 → *m/z* 302) (Figure 2).

Compound **17** (*m/z* 391.1331 $[M + H]^+$, $C_{21}H_{23}ClO_5$, 4.86 ppm, cos = 0.65) (Figure S30, SI section) shares the neutral and radical losses described for compound **12** and its analogs; however, some additional losses and structures were observed. The position of the positive charge on the carbonyl at C-8 in the ion at *m/z* 349 enables the simultaneous losses of CO and methyl radical, thus leading to the formation of a distonic ion *m/z* 306 (*m/z* 349 → *m/z* 306). Another observation was a second loss of H_2O from the fragment *m/z* 277 for the formation of the ion *m/z* 259 (Figure 3).

Compound **2** (*m/z* 353.1958 $[M + H]^+$, $C_{19}H_{28}O_6$, −1.70 ppm, cos = 0.68) (Figure S15, SI section) presents

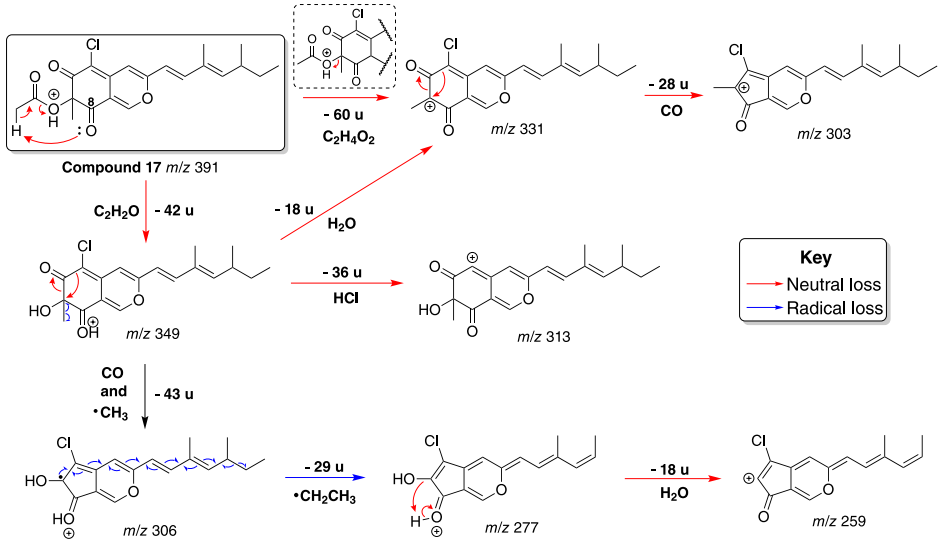

Figure 3. Fragmentation of compound **17**. Curved arrows indicate the proposed fragmentation mechanisms. Red arrows with full head indicate mechanisms that involve heterolytic cleavages and result in neutral losses. Blue arrows with half a head indicate mechanisms that involve homolytic cleavages and result in radical losses.

important modifications in its structure that favor a different fragmentation. Such modifications are the absence of double bond between C-1 and C-8a and presence of hydroxyl at C-7, C-8, C-11 and C-12. Its fragmentation route begins with a neutral loss of the aldehyde group ($C_5H_{10}O$, −86 u) (Figure 4), through heterolysis of the peripheral portion of the side chain and gives origin to the fragment *m/z* 267 and, from this, there is loss of H_2O (*m/z* 267 → *m/z* 249). From the ion *m/z* 249, there are competitive losses of CO and H_2O. The first is the loss of H_2O from the side chain by means of remote rearrangement of hydrogen, which gives origin to the fragment *m/z* 231 (*m/z* 249 → *m/z* 231) which, again loses H_2O, also by remote rearrangement of hydrogen,[64] thus leading to the formation of the ion *m/z* 213 (*m/z* 231 → *m/z* 213) and the loss of CO. From this, the tertiary cation *m/z* 185 (*m/z* 213 → *m/z* 185) originates, which is stabilized by resonance. The second fragmentation route is the loss of CO and formation of the ion *m/z* 221 (*m/z* 249 → *m/z* 221, favored) which then undergoes loss of H_2O, forming the ion *m/z* 203 (*m/z* 221 → *m/z* 203) and the subsequent loss of H_2O leads to the formation of the ion *m/z* 185 (*m/z* 203 → *m/z* 185) (Figure 4). Compound **1** (351.1799 $[M + H]^+$, $C_{19}H_{26}O_6$, −2.56 ppm, cos = 0.63) (Figure S14, SI section) was annotated as an analog of compound **2** and has a double bond between C-1 and C-8a. In its fragmentation route, the loss of H_2O through intramolecular rearrangement of the ion *m/z* 201, leads to the formation of the secondary cation *m/z* 183 (*m/z* 201 → *m/z* 183), which is stabilized by resonance (Figure 4). From compound **1**, compound **3** (*m/z* 391.2135 $[M + H]^+$, $C_{22}H_{30}O_6$, 3.58 ppm, cos = 0.74) (Figure S16, SI section) was annotated and, from this, compound **4** (*m/z* 425.1735 $[M + H]^+$, $C_{22}H_{29}ClO_6$,

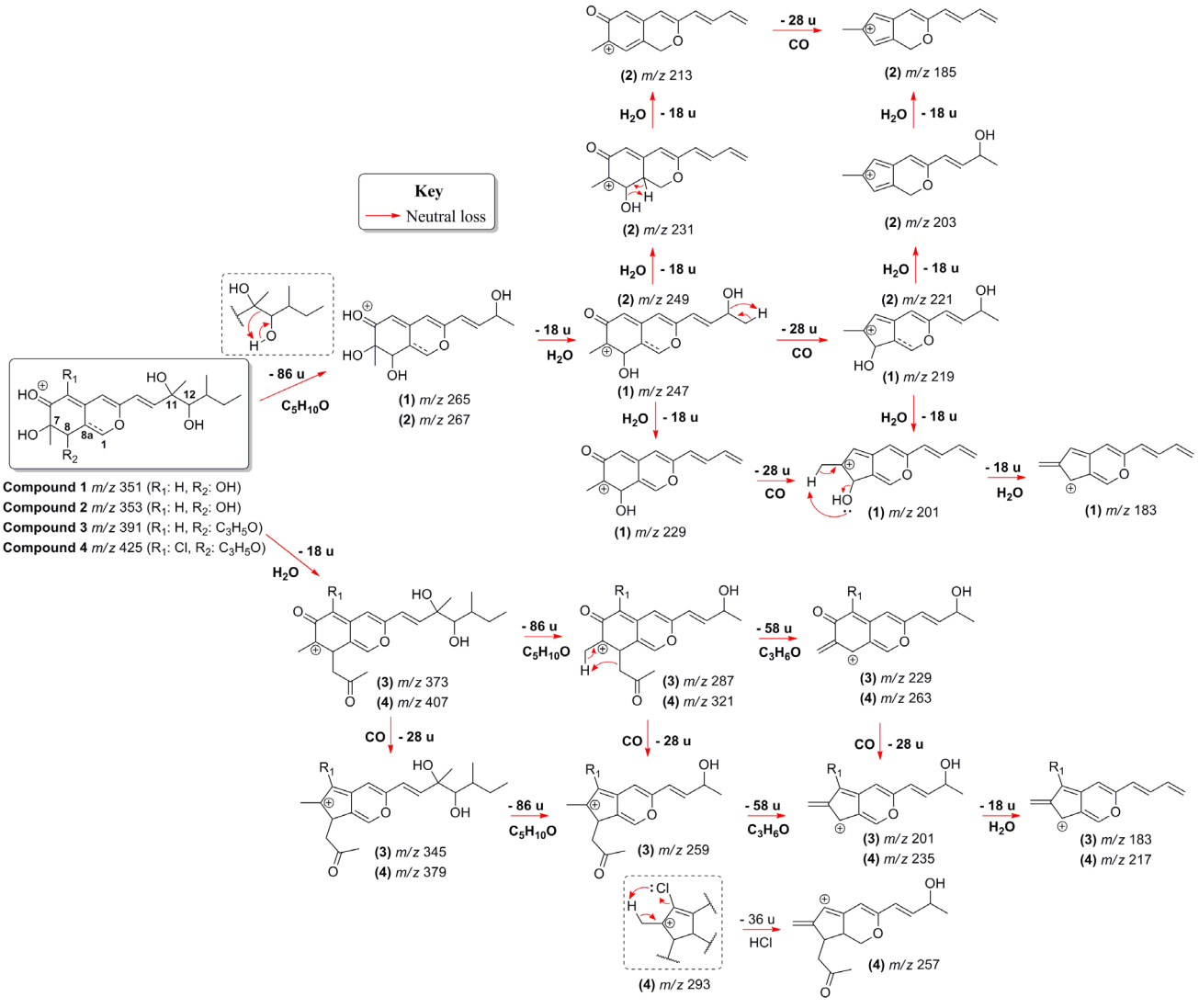

Figure 4. Fragmentation of compounds **1**, **2**, **3** and **4**. Curved arrows indicate the proposed fragmentation mechanisms. Red arrows with full head indicate mechanisms that involve heterolytic cleavages and result in neutral losses.

0.94 ppm, cos = 0.87) (Figure S17, SI section), which both have a ketone group at C-8. They share the same mass losses described for compound **2**; however, the fragmentation route begins with loss of H_2O and the presence of ketone group at C-8 allows the loss of propanone (C_3H_6O, −58 u) through intramolecular rearrangement that gives origin to a secondary cation. For compound **4**, HCl loss from the ion *m/z* 293 is proposed through intramolecular rearrangement, with formation of vinyl cation *m/z* 257 (Figure 4).

In the same group, compound **14** (*m/z* 357.2073 $[M + H]^+$, $C_{22}H_{28}O_4$, 1.96 ppm, cos = 0.76) (Figure S27, SI section) was annotated, which clusters with compounds **15** (*m/z* 383.1857 $[M + H]^+$, $C_{23}H_{26}O_5$, −0.26 ppm, cos = 0.76) (Figure S28, SI section) and **16** (*m/z* 381.1684 $[M + H]^+$, $C_{23}H_{24}O_5$, −4.72 ppm, cos = 0.70) (Figure S29, SI section). In the fragmentation route of compound **14** (Figure 5), the fragments result from neutral (H_2O, CO, HCl and propanone) and radical losses, which are widely described. However, a second loss of CO is proposed from the portion containing the ketone group at C-8 (Figure 5).

Compound **15** has a lactone ring as part of its structure and, in the molecular network, it clusters with compounds **14** (cos = 0.76) and **16** (cos = 0.79). Observations of the spectra of the product ions of compound **15** indicate two initial competitive fragmentation routes. The first and less favored route involves the loss of the ethyl radical with distonic ion formation *m/z* 354, which is stabilized by radical allylic isomerization. The second, more favored route has formation of the fragment *m/z* 339 from the loss of CO_2. All subsequent losses, following the fragmentation proposal, are the previously cited characteristic losses (Figure 6).

The proposed fragmentation route for compound **16** includes initial competitive losses of CO (*m/z* 381 → *m/z* 353) and ketene (*m/z* 381 → *m/z* 339) and final loss of CO_2 (*m/z* 267 → *m/z* 223) attributed to the resulting carboxylic acid group (Figure 7).

Compound **5** (*m/z* 373.2027 $[M + H]^+$, $C_{22}H_{28}O_5$, 3.22 ppm) (Figure S18, SI section), has an epoxide that is formed between C-11 and C-12. Grouped in molecular family A with compounds **3** (cos = 0.83) and **6** (*m/z* 417.1926 $[M + H]^+$, $C_{23}H_{28}O_7$, 3.12 ppm, cos = 0.70) (Figure S19, SI section). Its proposed fragmentation route (Figure 8) starts with initial neutral loss of H_2O (*m/z* 373 → *m/z* 355) and CO (*m/z* 355 → *m/z* 327). The latter undergoes successive hemolysis that results in the opening of the epoxide and loss of the ethyl radical (*m/z* 327 → *m/z* 298) and/or loss of propanone (*m/z* 327 → *m/z* 269). A second CO loss is also proposed (*m/z* 298 → *m/z* 270) (Figure 8).

Compound **6** has lactone ring as part of its structure and vicinal hydroxyls. It was annotated as an analog of compound **3** (cos = 0.77) and also clusters with compound **5** (cos = 0.70). As well as compound **3**, its fragmentation begins with neutral loss of the aldehyde group ($C_5H_{10}O$, −86 u) (Figure 9) via heterolysis of the peripheral portion of the chain (*m/z* 417 → *m/z* 331). With compound **5**, it shares the losses of CO_2 (*m/z* 303 → *m/z* 259) and propanone (*m/z* 259 → *m/z* 201) (Figure 9).

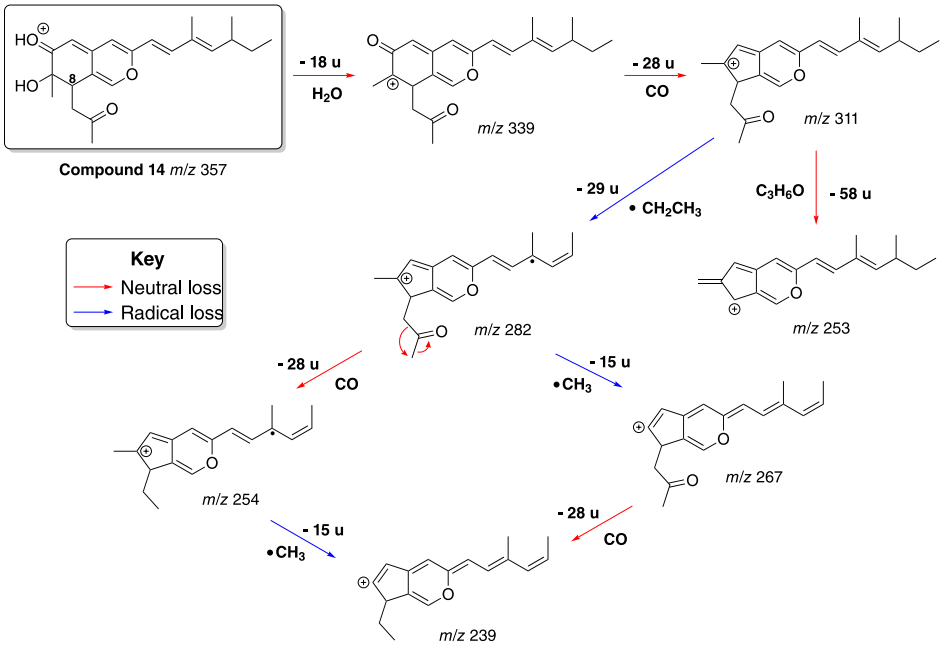

Figure 5. Fragmentation of compound **14**. Curved arrows indicate the proposed fragmentation mechanisms. Red arrows with a full head indicate mechanisms that involve heterolytic cleavages and result in neutral losses. Blue arrows indicate radical losses as a result of mechanisms involving homolytic cleavages.

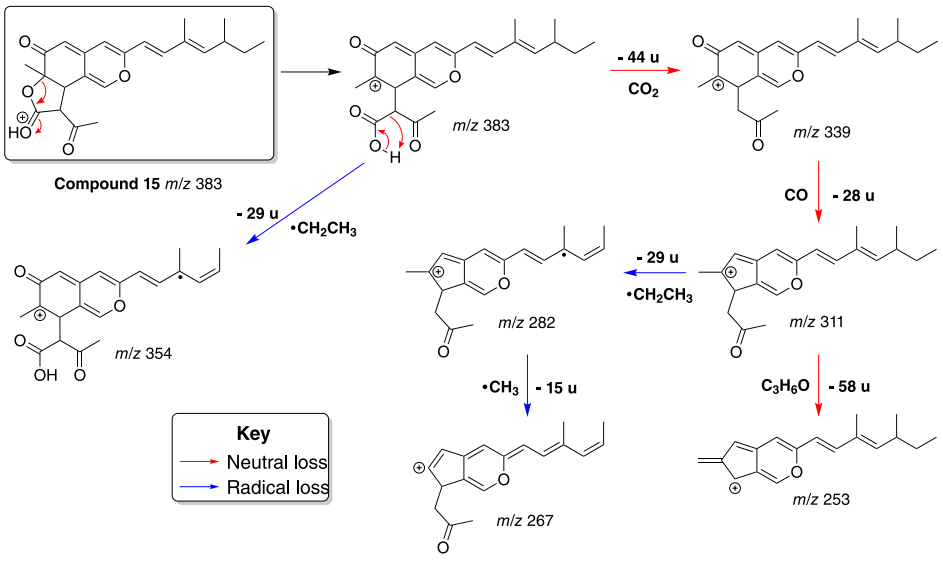

Figure 6. Fragmentation of compound **15**. Curved arrows indicate the proposed fragmentation mechanisms. Red arrows with full head indicate mechanisms that involve heterolytic cleavages and result in neutral losses. Blue arrows indicate radical losses as a result of mechanisms involving homolytic cleavages.

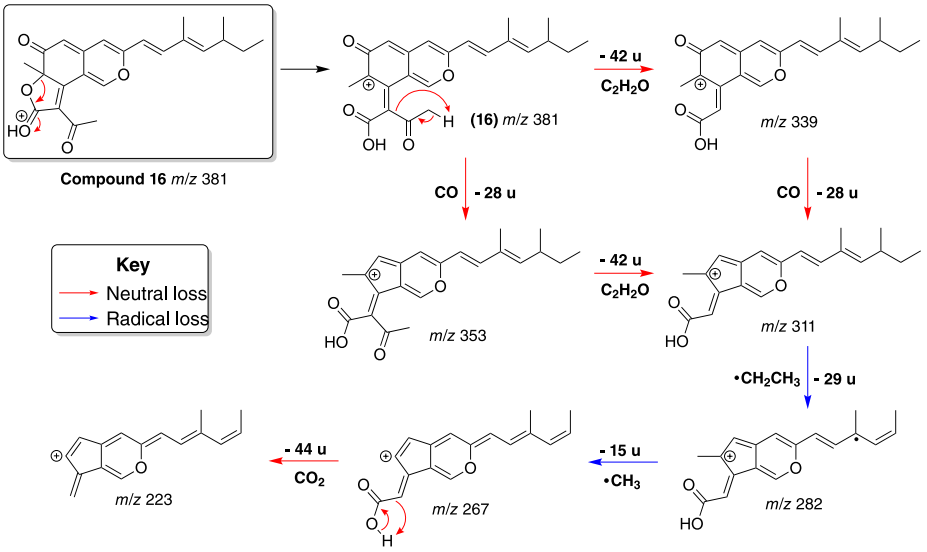

Figure 7. Fragmentation of compound **16**. Curved arrows indicate the proposed fragmentation mechanisms. Red arrows with full head indicate mechanisms that involve heterolytic cleavages and result in neutral losses. Blue arrows indicate radical losses as a result of mechanisms involving homolytic cleavages.

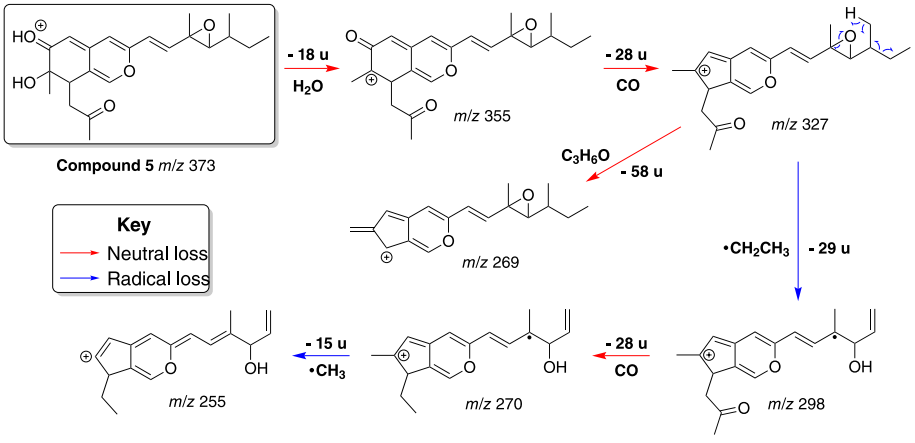

Figure 8. Fragmentation of compound **5**. Curved arrows indicate the proposed fragmentation mechanisms. Red arrows indicate neutral losses as a result of mechanisms involving heterolytic cleavages. Blue arrows with half a head indicate mechanisms that involve homolytic cleavages and result in radical losses.

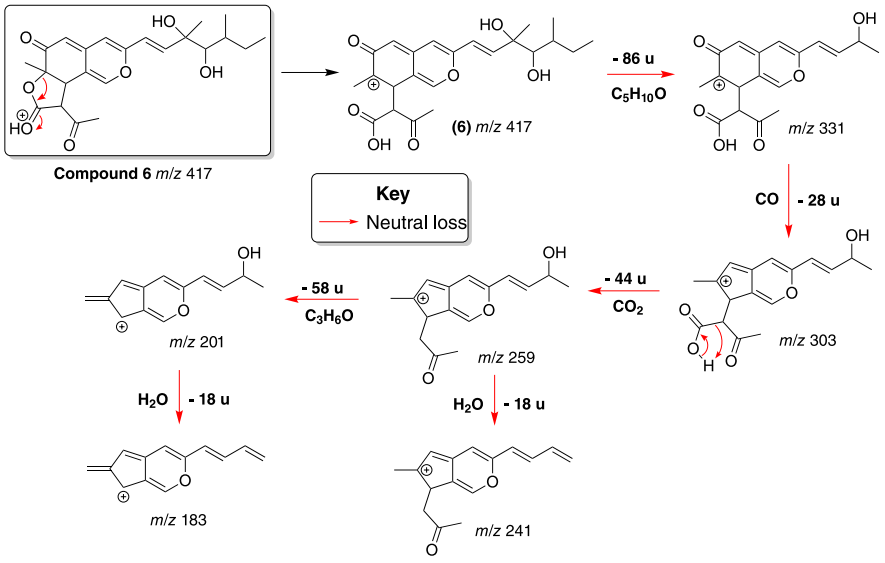

Figure 9. Fragmentation of compound **6**. Red arrows indicate neutral losses as a result of mechanisms involving heterolytic cleavages.

Conclusions

Penicillium meliponae is a recently discovered fungus of rare occurrence, and in this work it is reported for the first time as an endophytic fungus. The strain proved to be a prolific producer of polyketides belonging to the azaphilone class. The changes in the cultivation conditions served to explore the metabolic capacity of the species, generating a diversification in the structural skeletons of azaphilones, being its metabolic profile similar to other strains of fungi reported, showing promise in the production of pigments with biotechnological applications already reported, or even in the production of new metabolites.

By means of molecular networking and manual interpretation of MS/MS spectra, 17 azaphilones with sclerotiorin-type skeletons containing different structural substituents were identified, being the first report of the chemical profile of *P. meliponae*. Additionally, the diversification in the structures of the azaphilones showed that the strain is sensitive to changes in the composition of the culture medium and to presence of agitation, making it an excellent candidate for studies involving the production of azaphilones of interest through the diversification of conditions of cultivation.

Azaphilones are widely reported in the literature; however, the description of their behavior in the gas phase through fragmentation mechanisms are still scarce, and the present work, can contribute with the detailed chemistry of plausible fragmentation mechanisms that will serve as basis for future studies involving the identification/dereplication or characterization of new structural skeletons of azaphilones.

Supplementary Information

Supplementary information (high-resolution mass spectra) is available free of charge at https://jbcs.sbq.org.br as a PDF file.

Acknowledgments

The authors would like to thank the funding agencies Coordenação de Aperfeiçoamento de Pessoal de Nível Superior (CAPES - finance code 001), Conselho Nacional de Desenvolvimento Científico e Tecnológico (CNPq) and Fundação de Amparo à Pesquisa do Estado do Amazonas (FAPEAM). CNPq grant 435705/2018-0, CAPES-grant number 88881.200469/2018-01 (Procad AmazonMicro). Regarding FAPEAM, the authors would like to mention the following grants received: Amazonas Estratégico 004/2018/FAPEAM process No. 062.01303/2018 for H.H.F.K. and 062.01311/2018 for G.F.S.; CT&I Priority Areas 010/2021/FAPEAM process No. 01.02.016301.03429/2021-25 for H.H.F.K. and process No. 01.02.016301.03421/2021-00 for G.F.S.; and 008/2021 - POSGRAD 2021/FAPEAM process No. 01.02.016301.01964/2021 for H.H.F.K. and FAPESP 2020/08270-0 for L.S.M.

Author Contributions

EGP was responsible for investigation, data curation and writing original draft; MPS for investigation and data curation; TFS for data curation; CVAS for data curation; ALB for data curation and editing; FMAS for conceptualization, data curation and formal analysis; EVC for formal analysis and validation; LSM for formal analysis,

validation, writing-review and editing; MRF for investigation and data curation; ADLS for conceptualization, data curation and formal analysis; WHPP for data curation, formal analysis, validation, writing original draft, and writing-review and editing; GFS for data curation, formal analysis, validation and writing-review and editing; AQLS for conceptualization, data curation, formal analysis, funding acquisition, investigation and project administration and HHFK for conceptualization, data curation, formal analysis, funding acquisition, investigation, project administration, resources, validation, writing original draft, and writing-review and editing.

References

1. Antonelli, A.; Zizka, A.; Carvalho, F. A.; Scharn, R.; Bacon, C. D.; Silvestro, D.; Condamine, F. L.; *Proc. Natl. Acad. Sci. U.S.A.* **2018**, *115*, 6034. [Crossref]
2. Ritter, C. D.; Zizka, A.; Barnes, C.; Nilsson, R. H.; Roger, F.; Antonelli, A.; *Ecography* **2019**, *42*, 321. [Crossref]
3. Bardgett, R. D.; van der Putten, W. H.; *Nature* **2014**, *515*, 505. [Crossref]
4. Buscardo, E.; Souza, R. C.; Meir, P.; Geml, J.; Schmidt, S. K.; da Costa, A. C.; Nagy, L.; *Commun. Earth Environ.* **2021**, *2*, 55. [Crossref]
5. Blackwell, M.; *Am. J. Bot.* **2011**, *98*, 426. [Crossref]
6. Ritter, C. D.; Dunthorn, M.; Anslan, S.; de Lima, V. X.; Tedersoo, L.; Nilsson, R. H.; Antonelli, A.; *Ecol. Evol.* **2020**, *10*, 7509. [Crossref]
7. Koolen, H. H. F.; Soares, E. R.; da Silva, F. M. A.; de Almeida, R. A.; de Souza, A. D. L.; de Medeiros, L. S.; Rodrigues Filho, E.; de Souza, A. Q. L.; *Quim. Nova* **2012**, *35*, 771. [Crossref]
8. Celestino, J. R.; de Carvalho, L. E.; Lima, M. P.; Lima, A. M.; Ogusku, M. M.; de Souza, J. V. B.; *Process Biochem*. **2014**, *49*, 569. [Crossref]
9. da Silva-Filho, F. A.; de Souza, M. M. M.; Rezende, G. O.; da Silva, F. M. A.; da Cruz, J. C.; da Silva, G. F.; de Souza, A. D. L.; de Souza, A. Q. L.; *J. Braz. Chem. Soc.* **2021**, *32*, 1832. [Crossref]
10. Yadav, A. N.; Verma, P.; Kumar, V.; Sangwan, P.; Mishra, S.; Panjiar, N.; Gupta, V. K.; Saxena, A. K. In *New and Future Developments in Microbial Biotechnology and Bioengineering*, *Penicillium System Properties and Applications*; Gupta, V. K.; Rodriguez-Couto, S., eds.; Elsevier: Amsterdam, The Netherlands, 2018. [Crossref]
11. Houbraken, J.; Kocsubé, S.; Visagie, C. M.; Yilmaz, N.; Wang, X. C.; Meijer, M.; Kraak, B.; Hubra, V.; Samson, R. A.; Frisvad, J. C.; *Stud. Mycol.* **2020**, *95*, 5. [Crossref]
12. Yang, X.; Liu, J.; Mei, J.; Jiang, R.; Tu, S.; Deng, H.; Liu, J.; Yang, S.; Li, J.; *Mini-Rev. Med. Chem.* **2021**, *21*, 2000. [Crossref]
13. Osmanova, N.; Schultze, W.; Ayoub, N.; *Phytochem. Rev.* **2010**, *9*, 315. [Crossref]
14. Zhang, X.; Yin, Q.; Li, X.; Liu, X.; Lei, H.; Wu, B.; *Fitoterapia* **2022**, *163*, 105349. [Crossref]
15. Gao, J.-M.; Yang, S.-X.; Qin, J.-C.; *Chem. Rev.* **2013**, *113*, 4755. [Crossref]
16. Chen, C.; Tao, H.; Chen, W.; Yang, B.; Zhou, X.; Luo, X.; Liu, Y.; *RSC Adv.* **2020**, *10*, 10197. [Crossref]
17. Wang, X.; Sena Filho, J. G.; Hoover, A. R.; King, J. B.; Ellis, T. K.; Powell, D. R.; Cichewicz, R. H.; *J. Nat. Prod.* **2010**, *73*, 942. [Crossref]
18. Wang, W.-X.; Kusari, S.; Laatsch, H.; Golz, C.; Kusari, P.; Strohmann, C.; Kayser, O.; Spiteller, M.; *J. Nat. Prod.* **2016**, *79*, 704. [Crossref]
19. Wang, W.; Liao, Y.; Chen, R.; Hou, Y.; Ke, W.; Zhang, B.; Gao, M.; Shao, Z.; Chen, J.; Li, F.; *Mar. Drugs* **2018**, *16*, 61. [Crossref]
20. Zhou, Q.-Y.; Yang, X.-Q.; Zhang, Z.-X.; Wang, B.-Y.; Hu, M.; Yang, Y.-B.; Zhou, H.; Ding, Z.-T.; *Fitoterapia* **2018**, *130*, 26. [Crossref]
21. Wang, C.-Y.; Hao, J.-D.; Ning, X.-Y.; Wu, J.-S.; Zhao, D.-L.; Kong, C. J.; Shao, C.-L.; Wang, C.-Y.; *RSC Adv.* **2018**, *8*, 4348. [Crossref]
22. Yang, Z.-J.; Zhang, Y.-F.; Wu, K.; Xu, Y.-X.; Meng, X.-G.; Jiang, Z. T.; Ge, M.; Shao, L.; *Fitoterapia* **2020**, *145*, 104573. [Crossref]
23. Zhang, S.-P.; Huang, R.; Li, F.-F.; Wei, H.-X.; Fang, X.-W.; Xie, X.-S.; Lin, D.-G.; Wu, S. H.; He, J.; *Fitoterapia* **2016**, *112*, 85. [Crossref]
24. Li, X.; Tian, Y.; Yang, S.-X.; Zhang, Y.-M.; Qin, J.-C.; *Bioorg. Med. Chem. Lett.* **2013**, *23*, 2945. [Crossref]
25. Orfali, R. S.; Aly, A. H.; Ebrahim, W.; Rudiyansyah; Proksch, P.; *Phytochem. Lett.* **2015**, *13*, 234. [Crossref]
26. Giridharan, P.; Verekar, S. A.; Gohil, A. R.; Mishra, P. D.; Khanna, A.; Deshmukh, S. K.; *BioMed. Res. Int.* **2014**, ID 890904. [Crossref]
27. Wang, W.; Yang, J.; Liao, Y. Y.; Cheng, G.; Chen, J.; Cheng, X. D.; Qin, J. J.; Shao, Z.; *J. Nat. Prod.* **2020**, *83*, 1157. [Crossref]
28. Yu, H.; Sperlich, J.; Mándi, A.; Kurtán, T.; Dai, H.; Teusch, N.; Guo, Z. Y.; Zou, K.; Liu, Z.; Proksch, P.; *J. Nat. Prod.* **2018**, *81*, 2493. [Crossref]
29. Hsu, Y.-W.; Hsu, L.-C.; Liang, Y.-H.; Kuo, Y.-H.; Pan, T.-M.; *J. Agric. Food Chem.* **2011**, *59*, 4512. [Crossref]
30. Wu, H.-C.; Cheng, M.-J.; Wu, M.-D.; Chen, J.-J.; Chen, Y.-L.; Chang, H.-S.; *Phytochem. Lett.* **2019**, *31*, 242. [Crossref]
31. Zhang, Z. X.; Yang, X. Q.; Zhou, Q. Y.; Wang, B. Y.; Hu, M.; Yang, Y. B.; Zhou, H.; Ding, Z. T.; *Molecules* **2018**, *23*, 1816. [Crossref]
32. Mapari, S. A. S.; Thrane, U.; Meyer, A. S.; *Trends Biotechnol.* **2010**, *28*, 300. [Crossref]
33. Hebra, T.; Elie, N.; Poyer, S.; Van Elslande, E.; Touboul, D.; Eparvier, V.; *Metabolites* **2021**, *11*, 444. [Crossref]

34. Barbosa, R. N.; Bezerra, J. D. P.; Souza-Motta, C. M.; Frisvad, J. C.; Samson, R. A.; Oliveira, N. T.; Houbraken, J.; *Antonie van Leeuwenhoek* **2018**, *111*, 1883. [Crossref]
35. Doyle, J. J.; Doyle, J. L.; *Phytochem. Bull.* **1987**, *19*, 11.
36. *DNA Sequence Assembler*, version 4; Heracle BioSoft S.R.L., Romania, 2013.
37. GenBank, http://www.ncbi.nlm.nih.gov, accessed in January 2023.
38. Okonechnikov, K.; Golosova, O.; Fursov, M.; *Bioinformatics* **2012**, *28*, 1166. [Crossref]
39. Minh, B. Q.; Schmidt, H. A.; Chernomor, O.; Schrempf, D.; Woodhams, M. D.; Von Haeseler, A.; Lanfear, R.; *Mol. Biol. Evol.* **2020**, *37*, 1530. [Crossref]
40. Cyberinfrastructure for Phylogenetic Research (CYPRES), https://www.phylo.org, accessed in January 2023.
41. Nylander, J. A. A.; Ronquist, F.; Huelsenbeck, J. P.; Nieves-Aldrey, J. L.; *Syst. Biol.* **2004**, *53*, 47. [Crossref]
42. Rambaut, A.; *FigTree*, 1.3.1; Institute of Evolutionary Biology, University of Edinburgh, UK, 2009.
43. *CorelDRAW*, version 2020; Corel Corporation, Ottawa, Canada, 2021.
44. Bode, H. B.; Bethe, B.; Höfs, R.; Zeeck, A.; *ChemBioChem* **2002**, *3*, 619. [Crossref]
45. *Data Analysis*, version 4.2; Bruker Daltonik GmbH, Bremen, Germany, 2013.
46. Chambers, M. C.; Maclean, B.; Burke, R.; Amodei, D.; Ruderman, D. L.; Neumann, S.; Gatto, L.; Fischer, B.; Pratt, B.; Egertson, J.; Hoff, K.; Kessner, D.; Tasman, N.; Shulman, N.; Frewen, B.; Baker, T.A.; Brusniak, M.-Y.; Paulse, C.; Creasy, D.; Flashner, L.; Kani, K.; Moulding, C.; Seymour, S. L.; Nuwaysir, L. M.; Lefebvre, B.; Kuhlmann, F.; Roark, J.; Rainer, P.; Detlev, S.; Hemenway, T.; Huhmer, A.; Langridge, J.; Connolly, B.; Chadick, T.; Holly, K.; Eckels, J.; Deutsch, E. W.; Moritz, R. L.; Katz, J. E.; Agus, D. B.; MacCoss, M.; Tabb, D. L.; Mallick, P.; *Nat. Biotechnol*. **2012**, *30*, 918. [Crossref]
47. Global Natural Product Social Molecular Networking (GNPS), https://gnps.ucsd.edu/ProteoSAFe/status.jsp?task=06e87640023b4548a2ad7c670dc31caa, accessed in January 2023.
48. Wang, M.; Carver, J. J.; Phelan, V. V.; Sanchez, L. M.; Garg, N.; Peng, Y.; Nguyen, D. D.; Watrous, J.; Kapono, C. A.; Luzzatto-Knaan, T.; Porto, C.; Bouslimani, A.; Melnik, A. V.; Meehan, M. J.; Liu, W. T.; Crüsemann, M.; Dboudreau, P.; Esquenazi, E.; Sandoval-Calderón, M.; Kersten, R. D.; Pace, L. A.; Quinn, R. A.; Duncan, K. R.; Hsu, C. C.; Floros, D. J.; Gavilan, R, G.; Kleigrewe, K.; Northen, T.; Dutton, R. J.; Parrot, D.; Carlson, E. E.; Aigle, B.; Michelsen, C. F.; Jelsbak, L.; Sohlenkamp, C.; Pevzner, P.; Edlund, A.; McLean, J.; Piel, J.; Murphy, B. T.; Gerwick, L.; Liaw, C. C.; Yang, Y. L.; Humpf, H. U.; Maansson, M.; Keyzers, R. A.; Sims, A. C.; Johnson, A. R.; Sidebottom, A. M.; Sedio, B. E.; Klitgaard, A.; Larson, C. B.; Boya, C. A.; Torres-Mendoza, D.; Gonzalez, D. J.; Silva, D. B.; Marques, L. M.; Demarque, D. P.; Pociute, E.; O'Neill, E. C.; Briand, E.; Helfrich, E. J. H.; Granatosky, E. A.; Glukhov, E.; Ryffel, F.; Houson, H.; Mohimani, H.; Kharbush, J. J.; Zeng, Y.; Vorholt, J. A.; Kurita, K. L.; Charusanti, P.; McPhail, K. L.; Nielsen, K. F.; Vuong, L.; Elfeki, M.; Traxler, M. F.; Engene, N.; Koyama, N.; Vining, O. B.; Baric, R.; Silva, R. R.; Mascuch, S. J.; Tomasi, S.; Jenkins, S.; Macherla, V.; Hoffman, T.; Agarwal, V.; Williams, P. G.; Dai, J.; Neupane, R.; Gurr, J.; Rodríguez, A. M. C.; Lamsa, A.; Zhang, C.; Dorrestein, K.; Duggan, B. M.; Almaliti, J.; Allard, P. M.; Phapale, P.; Nothias, L. F.; Alexandrov, T.; Litaudon, M.; Wolfender, J. L.; Kyle, J. E.; Metz, T. O.; Peryea, T.; Nguyen, D. T.; VanLeer, D.; Shinn,P.; Jadhav, A.; Müller, R.; Waters, K. M.; Shi, W.; Liu, X.; Zhang, L.; Knight, R.; Jensen, P. R.; Palsson, B. O.; Pogliano, K.; Linington, R. G.; Gutiérrez, M.; Lopes, N. P.; Gerwick, W. H.; Moore, B. S.; Dorrestein, P. C.; Bandeira, N.; *Nat. Biotechnol.* **2016**, *34*, 828. [Crossref]
49. Shannon, P.; Markiel, A.; Ozier, O.; Baliga, N. S.; Wang, J. T.; Ramage, D.; Amin, N.; Schwikowski, B.; Ideker, T.; *Genome Res*. **2003**, *13*, 2498. [Crossref]
50. Mass Spectrometry Interactive Virtual Environment (MassIVE), https://massive.ucsd.edu/ProteoSAFe/static/massive.jsp, accessed in February 2023.
51. van Santen, J. A.; Jacob, G.; Leen Singh, A.; Aniebok, V.; Balunas, M. J.; Bunsko, D.; Carnevale Neto, F.; Castaño-Espriu, L.; Chang, C.; Clark, T. N.; Cleary Little, J. L.; Delgadillo, D. A.; Dorrestein, P. C.; Duncan, K. R.; Egan, J. M.; Galey, M. M.; Haeckl, F. P. J.; Hua, A.; Hughes, A. H.; Iskakova, D.; Khadilkar, A.; Lee, J.-H.; Lee, S.; LeGrow, N.; Liu, D. Y.; Macho, J. M.; McCaughey, C. S.; Medema, M. H.; Neupane, R. P.; O'Donnell, T. J.; Paula, J. S.; Sanchez, L. M.; Shaikh, A. F.; Soldatou, S.; Terlouw, B. R.; Tran, T. A.; Valentim, M.; van der Hooft, J. J. J.; Vo, D. A.; Wang, M.; Wilson, D.; Zink, K. E.; Linington, R. G.; *ACS Cent. Sc.* **2019**, *5*, 1824. [Crossref]
52. METLIN, https://metlin.scripps.edu, accessed in February 2023.
53. Pan, R.; Bai, X.; Chen, J.; Zhang, H.; Wang, H.; *Front. Microbiol.* **2019**, *10*, 294. [Crossref]
54. Fill, T. P.; Pallini, H. F.; Amaral, L. S.; da Silva, J. V.; Bidóia, D. L.; Peron, F.; Garcia, F. P.; Nakamura, C. V.; Rodrigues-Filho, E.; *J. Braz. Chem. Soc.* **2016**, *27*, 1444. [Crossref]
55. Xie, C.-L.; Liu, Q.; He, Z. H.; Gai, Y. B.; Zou, Z.-B.; Shao, Z.-Z.; Liu, G.-M.; Chen, H.-F.; Yang, X.-W.; *Bioorg. Chem.* **2021**, *108*, 104671. [Crossref]
56. Guo, W.; Peng, J.; Zhu, T.; Gu, Q.; Keyzers, R. A.; Li, D.; *J. Nat. Prod*. **2013**, *76*, 2106. [Crossref]
57. Fan, B.; Parrot, D.; Blümel, M.; Labes, A.; Tasdemir, D.; *Mar. Drugs* **2019**, *17*, 67. [Crossref]
58. Afshari, M.; Shahidi, F.; Mortazavi, S. A.; Tabatabai, F.; Es'haghi, Z.; *Nat. Prod. Res.* **2015**, *29*, 1300. [Crossref]
59. Gunasekaran, S.; Poorniammal, R.; *Afr. J. Biotechnol.* **2008**, *7*, 1894. [Crossref]

60. Pimenta, L. P.; Gomes, D. C.; Cardoso, P. G.; Takahashi, J. A.; *J. Fungi* **2021**, *7*, 541. [Crossref]
61. de Souza, M. P.: *Estudo Químico de Fungos Endofíticos Associados a Duguetia stelechantha e Rollinia sp.*; MSc Dissertation, Federal University of Amazonas, Brazil, 2012. [Link] accessed in January 2023
62. Aron, A. T.; Gentry, E. C.; McPhail, K. L.; Nothias, L. F., Nothias-Esposito, M.; Bouslimani, A.; Petras, D.; Gauglitz, J. M.; Sikora, N.; Vargas, F.; van der Hooft, J. J. J.; Ernst, M.; Kang, K. B.; Aceves, C. M.; Caraballo-Rodríguez, A. M.; Koester, I.; Weldon, K. C.; Bertrand, S.; Roullier, C.; Sun, K.; Tehan, R. M.; Boya, P. C. A.; Christian, M. H.; Gutiérrez, M.; Ulloa, A. M.; Tejeda Mora, J. A.; Mojica-Flores, R.; Lakey-Beitia, J.; Vásquez-Chaves, V.; Zhang, Y.; Calderón, A. I.; Tayler, N.; Keyzers, R. A.; Tugizimana, F.; Ndlovu, N.; Aksenov, A. A.; Jarmusch, A. K.; Schmid, R.; Truman, A. W.; Bandeira, N.; Wang, M.; Dorrestein, P. C.; *Nat. Protoc*. **2020**, *15*, 1954. [Crossref]
63. Sumner, L. W.; Amberg, A.; Barrett, D.; Beale, M. H.; Beger, R.; Daykin, C. A.; Fan, T. W. M.; Fiehn, O.; Goodacre, R.; Griffin, J. L.; Hankemeier, T.; Hardy, N.; Harnly, J.; Higashi, R.; Kopka, J.; Lane, A. N.; Lindon, J. C.; Marriott, P.; Nicholls, A. W.; Reily, M. D.; Thaden, J. J.; Viant, M. R.; *Metabolomics* **2007**, *3*, 211. [Crossref]
64. Demarque, D. P.; Crotti, A. E. M.; Vessecchi, R.; Lopes, J. L. C.; Lopes, N. P.; *Nat. Prod. Rep.* **2016**, *33*, 432. [Crossref]
65. Gabelica, V.; Pauw, E. D.; *Mass Spectrom. Rev.* **2005**, *24*, 566. [Crossref]
66. Seto, C.; Grossert, J. S.; Waddell, D. S.; Curtis, J. M.; Boyd, R. K.; *J. Am. Soc. Mass Spectrom.* **2001**, *12*, 571. [Crossref]
67. Tomazela, D. M.; Sabino, A. A.; Sparrapan, R.; Gozzo, F. C.; Eberlin, M. N.; *J. Am. Soc. Mass Spectrom.* **2006**, *17*, 1014. [Crossref]
68. Neta, P.; Godugu, B.; Liang, Y.; Simón-Manso, Y.; Yang, X.; Stein, S. E.; *Rapid Commun. Mass Spectrom.* **2010**, *24*, 3271. [Crossref]
69. Tang, J.-L.; Zhou, Z.-Y.; Yang, T.; Yao, C.; Wu, L.-W.; Li, G.-Y.; *J. Agric. Food Chem.* **2019**, *67*, 2175. [Crossref]

Submitted: September 2, 2022
Published online: February 28, 2023